

Analysis of Ice Absorption Features toward YSO Candidates using *AKARI*

TOMOYUKI KIMURA,¹ TAKASHI ONAKA,¹ ITSUKI SAKON,¹ AND TAKASHI SHIMONISHI²

¹*Department of Astronomy, Graduate School of Science, The University of Tokyo, 7-3-1 Hongo, Bunkyo-ku, Tokyo 113-0033, Japan*

²*Frontier Research Institute for Interdisciplinary Sciences, Tohoku University, Aramaki-zaaoba 6-3, Aoba-ku, Sendai, Miyagi, 980-8578, Japan*

ABSTRACT

We serendipitously discovered two young stellar object (YSO) candidates using the slit-less spectroscopic mode of the InfraRed Camera (IRC) on board *AKARI*. They are not associated with any known star-forming regions in the Galactic plane. Absorption bands of molecular species, including solid phase H₂O, CO₂, CO, and possibly gas phase CO, are seen in the spectra of both sources. In one of the sources, absorption bands of crystalline H₂O, XCN, organics, and silicates are also seen. These results suggest that the objects are highly embedded class I YSOs or class II YSOs with an edge-on disk. However, their bluer color than typical YSOs and non-detection at far-infrared are not reconciled with expected spectral energy distributions of YSOs. Confirmation of these objects as YSOs will have a significant impact on the YSO study because it will suggest that a number of YSOs may have eluded detection in past infrared photometric surveys and could renew the census of YSOs on a galactic scale and their evolutionary tracks. The constraint of the properties of warm CO gas from high resolution spectroscopy in the M-band is crucial to reveal the true nature of the objects.

Keywords: astrochemistry – circumstellar matter – stars: evolution – dust extinction – infrared: stars

1. INTRODUCTION

Understanding of the properties of ice species in the envelopes and circumstellar disks of Young Stellar Objects (YSOs) is vital for the study of star-formation (e.g., Gibb et al. 2004; Boogert et al. 2004; Dartois 2005), but the sample size for which detailed study has been made is still limited. Color-color diagrams in the infrared are often employed in the photometric search of YSOs and the efficient selection of YSO candidates is becoming one of the important issues (e.g., Whitney et al. 2008; Gruendl & Chu 2009). We found two atypical YSO candidates in serendipitous slit-less spectroscopy with the InfraRed Camera (IRC) on board *AKARI* (IRC; Onaka et al. 2007). We discuss here the nature of these objects.

2. OBSERVATION & RESULTS

Slit-less spectroscopic pointing observations to of the Galactic plane were made with the grism mode of the *AKARI*/IRC as part of *AKARI* phase 2 mission in 2007 for the investigations of ISMs in our Galaxy. The present observations employed slit-less spectroscopic modes of NG (2.5–5.0 μm , $R(= \lambda/\Delta\lambda) \sim 100$), SG1 (4.6–9.2 μm , $R \sim 40$), and SG2 (7.2–13.4 μm , $R \sim 30$) of the IRC. Out of 46 areas observed, two young stellar object (YSO) candidates (Object 1: $\alpha(\text{J2000})=14:04:13.3$, $\delta(\text{J2000})=-61:12:40.0$ and Object 2: $\alpha(\text{J2000})=14:04:20.2$, $\delta(\text{J2000})=-61:12:49.7$) that show deep ice absorption were found in a $10' \times 10'$ area in the Crux region from the image taken on Feb 12 2007 (see Figure 1). 2MASS, WISE, *Spitzer* GLIMPSE, and *AKARI* photometric data are also available for both objects. However, due to the very blue colors of the infrared (see below) they have not been identified as YSOs.

We apply the standard data reduction and extract sources from the slit-less spectroscopic images using the IRC spectroscopic data reduction toolkit of version 20150331 (e.g., Ohyama et al. 2007). Combining the spectra taken by the NG, SG1, and SG2 modes, we obtain near- to mid- infrared spectral energy distributions (SEDs) of both sources (Figure 2). Note that the 2.5–4 μm and the region longer than 5 μm of Object 2 are not reliable due to overlaps with neighboring objects.

3. ANALYSIS & DISCUSSION

We first assume appropriate continuum for each object. For wavelengths shorter than 5 μm of both objects, we apply a second order polynomial fit to the spectrum where no absorption features are expected, while we assume a 1000K blackbody for the spectrum longer than 5 μm of Object 1. Then we derive the optical depth profile for each absorption feature and fit it with the laboratory data for the ice species (Ehrenfreund et al. 1996; Öberg et al. 2007; Bisschop et al. 2007) and Gaussian profiles for the unidentified features (e.g., $\sim 4.4 \mu\text{m}$), estimating the column densities. The optical depth and fitting results are shown in Figure 3 and the derived column densities are summarized in Table 1.

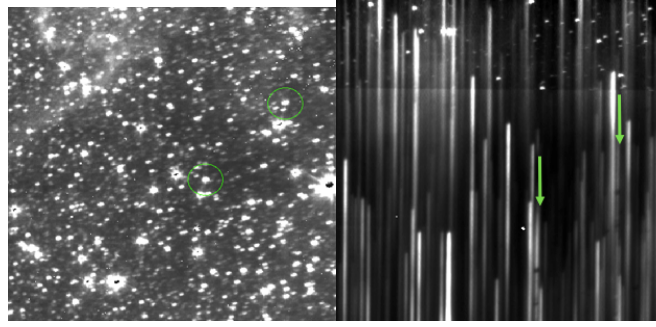


Figure 1. (left) AKARI/IRC pointing observation image of the objects in the NIR channel. Two point sources indicated by the green circles are the targets in this study. The left one is Object 1 and the right one is Object 2. The field-of-view (FoV) is $10' \times 10'$. (right) Spectroscopic image of the same region obtained with the NG slit-less mode. Objects 1 and 2 are indicated by the green arrows.

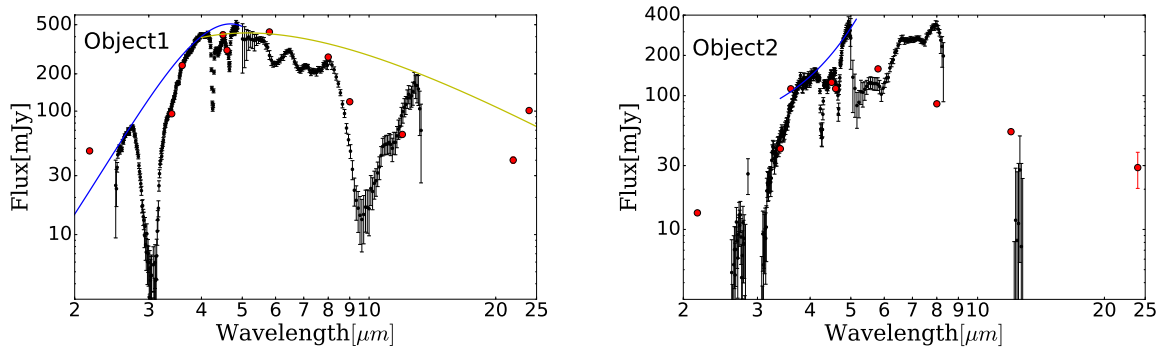


Figure 2. Spectral energy distribution (SED) of Object 1 (left) and Object 2 (right). The black dotted lines with the error bars show the observed SEDs and the red dots indicate photometric data points of 2MASS, GLIMPSE, and WISE. Solid lines indicate the continua assigned to each spectral region (blue: 2nd polynomial, yellow: 1000K Blackbody).

Table 1. Abundance of ice and molecular species in Objects 1 and 2 in units of 10^{17}cm^{-2} and comparison with typical YSOs

Object	N(H ₂ O)	N(CH ₃ OH)	N(CO ₂)	N(CO ice)	N(CO gas)	N(XCN)	N(HCOOH)
Object 1	54.2 ± 2.7	< 4	6.3 ± 0.3	11.9 ± 2.3	59 ± 23 (350K)	1.8 ± 0.6	< 6
Object 2	no data	no data	5.9 ± 0.2	13.2 ± 0.9	98 ± 21 (150K)	< 0.6	no data
Object 1 ^a	100	< 7	12	22	110	3.3	< 11
Massive YSO ^b	100	9	19	7	no data	0.6	4
Low-mass YSO ^b	100	6	28	21	no data	0.6	non detection
Background star ^b	100	8	26	25	no data	non detection	non detection

^aNormalized to the H₂O abundance (=100)

^bNormalized abundance of typical YSOs from Boogert et al. (2015)

The absorption features seen in 4.5–4.7 μm towards Object 1 can be interpreted as a combination of CO gas of 350K, CO ice, and XCN and towards Object 2 as CO gas of 150K and CO ice. The spectrum of Object 1 also shows deep absorption of H₂O ice, which may have crystalline form, small 6–8 μm features that are attributed to various organic ices (Boogert et al. 2015), and deep $\sim 10 \mu\text{m}$ silicate absorption (not fitted).

CO gas is a tracer of a warm environment (\sim several 100s K), and XCN and crystalline H₂O are of thermal processing. Their presence thus supports that both objects are YSOs. The derived high column densities of ice species and the presence of CO gas and XCN imply that the objects may be an embedded Class I massive YSO or a Class II YSO with an edge-on disk to a certain extent ($i \sim 70^\circ$, Pontoppidan et al. 2005). However, their SED peaks at around 4 μm , which is atypical to embedded YSOs (Figure 2). In addition, the Herschel Infrared Galactic Survey (Hi-GAL; Molinari et al. 2016) does not detect any far-infrared emission towards Object 1 at 70 and 170 μm . As shown in Figure 5, their color in infrared is unusual due to extremely low flux at longer wavelengths. These facts suggest a possibility of a normal star behind a dense cloud. Figure 4 shows the YSO SED model (Robitaille et al. 2007) fitting result. It suggests that they may be nearby

ANALYSIS OF ICE ABSORPTION FEATURES TOWARD YSO CANDIDATES USING AKARI

P25 - 3

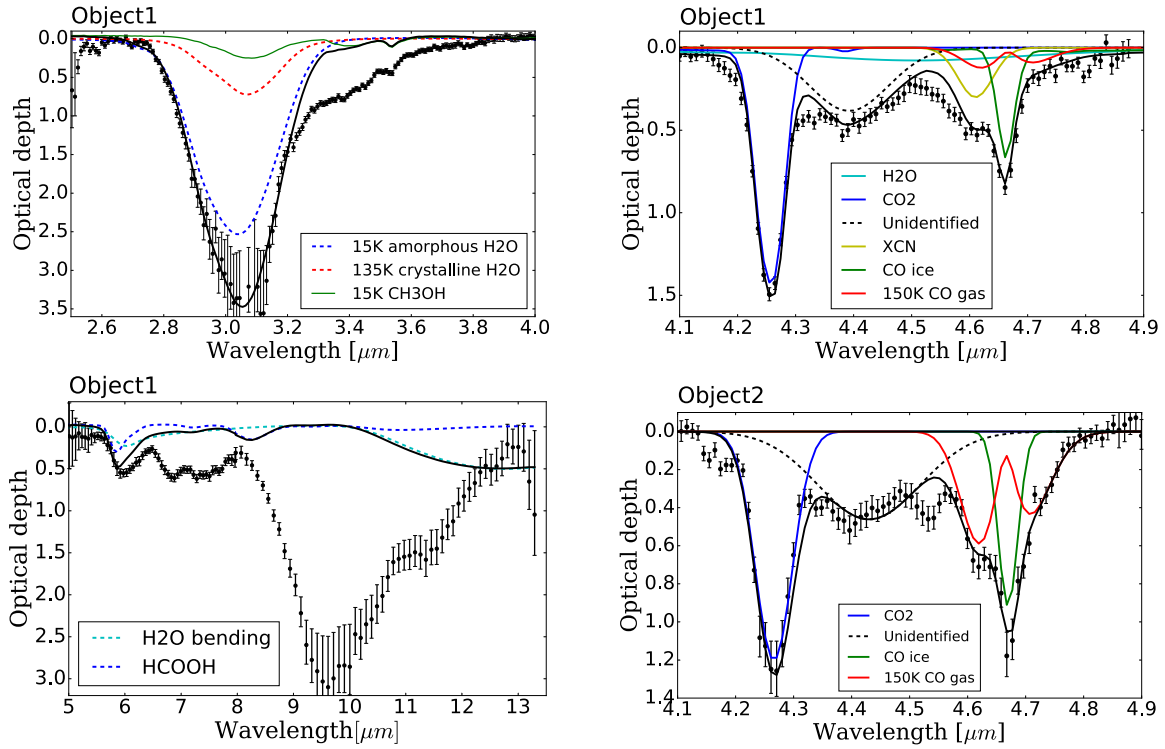


Figure 3. Results of fitting of the absorption features. The black solid lines indicate the summation of several absorption features. A Gaussian feature (*unidentified*; the black dashed line) is added to fit to the residual absorption near $4.4\mu\text{m}$ in both objects. The spectra of $2.5\text{--}4\mu\text{m}$, $4\text{--}5\mu\text{m}$, and $5\text{--}13\mu\text{m}$ of Object 1, that of $2.5\text{--}4\mu\text{m}$ of Object 2 are shown in the top left, top right, and bottom left, and bottom left panels, respectively.

($\sim 0.1\text{kpc}$) and heavily attenuated ($A_V \sim 50$) background stars. However, there is no known CO cloud in this region (Dame et al. 1987) and no clear nebulosity is seen in the $3\mu\text{m}$ image. A_V in this region is also not very high ($A_V < \sim 10$, Dobashi et al. 2005). Thus, there is no supporting evidence for the background star hypothesis either.

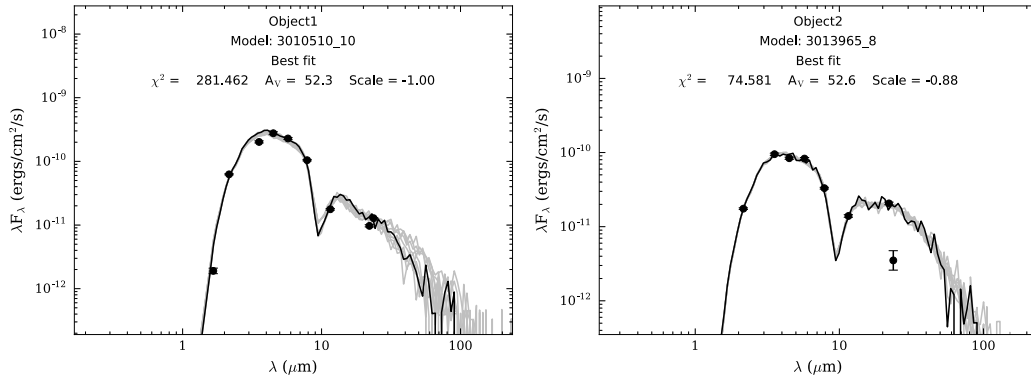


Figure 4. YSO SED model fitting result. The SED models and fitting tools are taken from Robitaille et al. (2007). The black dots indicate the input observed flux and the solid lines show the selected model SEDs that fit to the observed data (top 10 out of 200,000 model YSOs with different parameters are shown). The best-fit SED is shown by the black solid line and other fitted models are by the gray lines. The parameters of the best-fit model YSO are given in the figure (χ^2 , interstellar extinction A_V , and the distance from the earth (distance = $10^{\text{scale}}[\text{pc}]$)).

As shown in Figure 5, both objects are located outside of the region in an infrared color-color diagram, where known YSOs are present or where objects have not been identified as YSOs. If the two objects are proved to be truly YSOs, past search may have missed similar YSOs. No detection in the far-infrared will also raise a challenge of modeling of the objects and their evolutionary stage since deep ice absorption requires a large optical depth of obscuring dust that must emit in the far-infrared (Crapsi et al. 2008). If they turn out to be background stars, it suggests the presence of very localized dense clouds in the ISM, which will also have a significant impact on our understanding of the ISM.

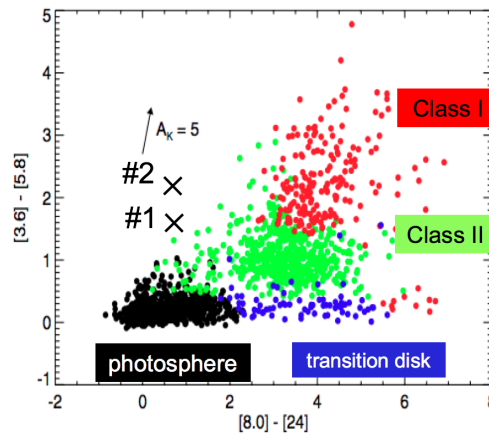


Figure 5. [3.6] - [5.8] vs. [8.0] - [24] *Spitzer* IRAC and MIPS color-color diagram of YSOs by [Beerer et al. \(2010\)](#). The dots represent YSOs candidates in the Cygnus X region. Each color dot represents different evolutionary stages of YSOs (red: Class I YSO, green: Class II YSO, blue: transition disk, black: naked star). The classification criteria presented in [Gutermuth et al. \(2008\)](#) are used. The positions of the objects in this study are plotted by the crosses.

4. SUMMARY

We discovered two YSO candidates in the Galactic plane with *AKARI*/IRC slit-less spectroscopic survey. The presence of absorption features of various ices, silicates, and warm CO gas suggests that they are massive YSOs with thick envelopes or edge-on disks. On the other hand, the unusual IRAC8.0-MIPS24 color and non-detection in the FIR suggest that they might be evolved YSOs, background stars, or OH/IR stars. The apparent absence of molecular clouds in the region does not support the background star hypothesis. Several contradicting observational characteristics for these objects prevent us from drawing a clear conclusion from the presently available data. Further detailed observations in the infrared are definitely needed for the understanding of their true nature.

ACKNOWLEDGMENTS

This work is based on observations with *AKARI*, a JAXA project with the participation of ESA. It has made use of the NASA/IPAC Infrared Science Archive, which is operated by the Jet Propulsion Laboratory, California Institute of Technology, under contract with the National Aeronautics and Space Administration. This research is supported by Grant-in-Aid for Scientific Research from the Japan Society for the Promotion of Science (16H00934).

REFERENCES

- Beerer, I. M., et al. 2010, *ApJ*, 720, 679
 Bisschop, S. E., Fuchs, G. W., Boogert, A. C. A., van Dishoeck, E. F., & Linnartz, H. 2007, *A&A*, 470, 749
 Boogert, A. C. A., Gerakines, P. A., & Whittet, D. C. B. 2015, *ARA&A*, 53, 541
 Boogert, A. C. A., et al. 2004, *ApJS*, 154, 359
 Crapsi, A., Van Dishoeck, E. F., Hogerheijde, M. R., Pontoppidan, K. M., & Dullemond, C. P. 2008, *A&A*, 486, 245
 Dame, T. M., et al. 1987, *ApJ*, 322, 706
 Dartois, E. 2005, *SSRv*, 119, 293
 Dobashi, K., Uehara, H., Kandori, R., Sakurai, T., Kaiden, M., Umemoto, T., & Sato, F. 2005, *PASJ*, 57, 1
 Ehrenfreund, P., Boogert, A., Gerakines, P., Jansen, D., Schutte, W., Tielens, A., & van Dishoeck, E. 1996, *A&A*, 315, L341
 Gibb, E. L., Whittet, D. C. B., Boogert, A. C. A., & Tielens, A. G. G. M. 2004, *ApJS*, 151, 35
 Gruendl, R. A., & Chu, Y.-H. 2009, *ApJS*, 184, 172
 Gutermuth, R. A., et al. 2008, *ApJ*, 674, 336
 Molinari, S., et al. 2016, *A&A*, 591, A149
 Öberg, K. I., Fraser, H. J., Boogert, A. C. A., Bisschop, S. E., Fuchs, G. W., van Dishoeck, E. F., & Linnartz, H. 2007, *A&A*, 462, 1187
 Ohyama, Y., et al. 2007, *PASJ*, 59, S411
 Onaka, T., et al. 2007, *PASJ*, 59, 401
 Pontoppidan, K. M., Dullemond, C. P., van Dishoeck, E. F., Blake, G. A., Boogert, A. C. A., Evans, II, N. J., Kessler-Silacci, J. E., & Lahuis, F. 2005, *ApJ*, 622, 463
 Robitaille, T. P., Whitney, B. A., Indebetouw, R., & Wood, K. 2007, *ApJS*, 169, 328
 Whitney, B. A., et al. 2008, *AJ*, 136, 18